ARTICLE IN PRESS

Disentangling the low-energy states of the major light-harvesting complex of plants and their role in photoprotection ☆

Tjaart P.J. Krüger [a,b,*], Cristian Ilioaia [b,c], Matthew P. Johnson [d], Alexander V. Ruban [e], Rienk van Grondelle [b,**]

[a] Department of Physics, Faculty of Natural and Agricultural Sciences, University of Pretoria, Private bag X20, Hatfield 0028, South Africa
[b] Department of Physics and Astronomy, Faculty of Sciences, VU University, De Boelelaan 1081, 1081 HV Amsterdam, The Netherlands
[c] Institute of Biology and Technology of Saclay, CEA, UMR 8221 CNRS, University Paris Sud, CEA Saclay, 91191 Gif-sur-Yvette, France
[d] Department of Molecular Biology and Biotechnology, University of Sheffield, Sheffield S10 2TN, UK
[e] School of Biological and Chemical Sciences, Queen Mary University of London, Mile End Road, London E1 4NS, UK

ARTICLE INFO

ABSTRACT

The ability to dissipate large fractions of their absorbed light energy as heat is a vital photoprotective function of the peripheral light-harvesting pigment–protein complexes in photosystem II of plants. The major component of this process, known as qE, is characterised by the appearance of low-energy (red-shifted) absorption and fluorescence bands. Although the appearance of these red states has been established, the molecular mechanism, their site and particularly their involvement in qE are strongly debated. Here, room-temperature single-molecule fluorescence spectroscopy was used to study the red emission states of the major plant light-harvesting complex (LHCII) in different environments, in particular conditions mimicking qE. It was found that most states correspond to peak emission at around 700 nm and are unrelated to energy dissipative states, though their frequency of occurrence increased under conditions that mimicked qE. Longer-wavelength emission appeared to be directly related to energy dissipative states, in particular emission beyond 770 nm. The ensemble average of the red emission bands shares many properties with those obtained from previous bulk in vitro and in vivo studies. We propose the existence of at least three excitation energy dissipating mechanisms in LHCII, each of which is associated with a different spectral signature and whose contribution to qE is determined by environmental control of protein conformational disorder. Emission at 700 nm is attributed to a conformational change in the Lut 2 domain, which is facilitated by the conformational change associated with the primary quenching mechanism involving Lut 1.

1. Introduction

The main function of the extended network of membrane-bound light-harvesting antennae in plants is to efficiently capture photons and rapidly transfer the excitation energy to the reaction centre, where the initial energy stabilisation takes place [1–3]. The efficiency of excitation energy transfer is strongly influenced by the presence of energy traps. The plant photosystem (PS) II has the intriguing ability to tune the amount of trapping according to the external environment.

In particular, when exposed to a demanding environment, such as high levels of irradiation, a large fraction of excitation energy is non-photochemically dissipated as heat in PS II to protect the reaction centre from photoinhibition. Because the chlorophyll (Chl) a pigments are the main contributors to the lowest exciton states of these antenna complexes, the extent of thermal energy dissipation can be monitored by a reduction in the Chl a fluorescence quantum yield and, for isolated antennae, the fluorescence intensity. This negative feedback regulatory function is hence generally referred to as non-photochemical quenching (NPQ) of Chl a fluorescence.

The major component of NPQ, known as qE, is energy dependent and reversible and is activated by the transmembrane electrochemical gradient caused by an accumulation of protons on the luminal side. The low luminal pH induces the xanthophyll cycle, during which violaxanthin (Vio) in the PS II antennae is enzymatically converted into zeaxanthin (Zea) [4], protonates the Lhcb and PsbS proteins [5,6], and causes the antenna complexes to rearrange and aggregate within the membrane [7].

There is considerable evidence that qE occurs in the PS II peripheral antenna complexes [8–10]. The genes coding for these proteins (Lhcb1–6) belong to the light-harvesting complex (Lhc) multigene family,

which also contains the antenna complexes of PS I, often labelled by Lhca. The most frequent assembly of Lhcb proteins consists of heterotrimers of Lhcb1–3 and is commonly known as the major, LHCII complexes. The minor antennae, Lhcb4–6, exist naturally as monomers and in smaller numbers. The proteins Lhcb1–6 all coordinate Chl a, Chl b, and a few xanthophyll pigments in different amounts but at similar sites. Without the protein scaffold, the high Chl concentration of ~0.3 M [11] would give rise to an almost complete fluorescence quenching [12]. It is therefore not surprising that slight perturbations of these complexes may open up various dissipation pathways, a property which significantly complicates the study of qE and which may explain why several possible molecular mechanisms for qE have been put forward.

Formation of qE is accompanied by various spectroscopic changes. One characteristic marker is the appearance of low-energy (red) components in the absorption and fluorescence spectra of the PS II peripheral antennae [13–16]. The red emission and the degree of qE are considerably enhanced when protein aggregates are formed [17]. For the aggregates the yield of red emission is very low at room temperature, but increases dramatically at cryogenic temperatures [15,17], forming a prominent band near 700 nm (often labelled by F700) in addition to the characteristic room-temperature emission band near 680 nm (F680). The F700 emission at 77 K is often used as a signature for aggregation of light-harvesting proteins [18]. These observations have frequently been a basis for considering the F700 states to be directly involved with the major molecular mechanism of qE and to originate from inter-trimer interactions [14,16,19–22]. However, F700 emission was also observed at 77 K from quenched LHCII trimers in arrangements where protein aggregation was prevented [23,24], indicating that the associated states are intrinsic to an LHCII trimer. Furthermore, early transient absorption studies have indicated that the long-wavelength pigment pools of LHCII aggregates are not quenched and have long lifetimes at low temperatures [25,26].

The most plausible explanation for the large energy shifts related to the F700 state involves the formation of a charge-transfer (CT) state that mixes with one or more exciton states, *i.e.*, a CT state with a pronounced excited-state character. Several observations support the involvement of a CT state: (i) the broad spectral shapes cannot be explained by pure exciton states; (ii) fluorescence Stark measurements on LHCII aggregates indicated a strong response of different low-energy states to an externally applied electrical field [27]; (iii) the very low hole-burning efficiency of LHCII aggregates beyond 683 nm was related to strong electron–phonon coupling due to a CT-state character [28]; and (iv) modelling of single-molecule (SM) spectra of LHCII trimers indicated that only relatively small spectral variations (*i.e.*, within ~10 nm of F680) can be explained by pigment site-energy disorder, while larger red shifts demand the presence of special states [29]. A CT state alone is non-radiative, but its mixing with an exciton state results in fluorescence emission that corresponds to a large reorganisation shift and involves a large contribution of higher vibronic substates [30]. Indeed, SM studies have indicated that Lhcb complexes can behave spectroscopically like Lhca complexes [31], the latter of which are characterised by low-energy emission with many properties related to the F700 state and which was shown to originate from a mixed exciton–CT state [30,32,33].

The location and molecular mechanism of qE are still under debate. Various studies have suggested that LHCII trimers are a key player [20,24,34–36]. Each monomeric subunit of these complexes contains eight Chl a's, six Chl b's, two luteins (Lut), one neoxanthin (Neo) and either Zea or Vio at a peripheral site. One molecular mechanism of qE was proposed based on femtosecond transient absorption spectroscopy of solubilised aggregates of LHCII trimers [36]. Although the transient absorption study was performed on aggregates, the suggested mechanism occurs on the level of a trimer. It was found that under qE conditions the S_1 state of Lut 1 (nomenclature as in [37]) is populated by direct energy transfer from the terminal emitter Chls, after which the S_1 state decays non-radiatively by rapid internal conversion [36].

Alternatively, a few groups have advocated a prominent role of the minor antenna complexes in qE after indications had been found that Zea–Chl or Lut–Chl CT states in some of these complexes accompanied energy dissipation [20,38–40].

By investigating single, isolated LHCII trimers it was demonstrated that these complexes frequently adopt states associated with considerable non-radiative energy dissipation when illuminated continuously [29,41–43]. Although the rapid and reversible fluorescence intensity changes (a phenomenon generally known as fluorescence intermittency or fluorescence blinking) are common for virtually all fluorescing systems, they retain various unique features for LHCII [44]. One such element is that quenched states are significantly enhanced when the experimental environment mimics conditions related to qE *in vivo* [45], a behaviour found to be specific for LHCII trimers [46]. It was considered that the combined fluorescence signal of millions or billions of simultaneously excited complexes in an *in vivo* or *in vitro* environment can be averaged into a single intensity level. Environmentally induced changes in this intensity reflect the extent of qE and can be compared with the time- and population-averaged intensity of numerous SM time traces. As such it was proposed that a major component of qE occurs in LHCII trimers and shares the same primary molecular mechanism with fluorescence blinking for these complexes. The correlation between qE and fluorescence blinking for LHCII trimers is supported by a quantitative simulation of their experimental blinking behaviour [47,48]. This conceptual model is based on the dynamic self-organisation of the intrinsic LHCII structure and describes the protein conformational diffusion in the vicinity of the lowest exciton state. The dynamics in this region – the Lut 1 domain – were consequently associated with the qE mechanism proposed in Ref. [36]. These findings indicate that the local environment of an LHCII complex can regulate its protein conformational disorder, considering that this disorder is manifested by the intermittent intensity dynamics.

SM studies have indicated the intrinsic capability of LHCII to switch its fluorescence abruptly not only in intensity but also in energy [29,43]. The rich variety of fluorescence profiles showed various distinct characteristics as compared to those from other photosynthetic complexes [49–54]. The most common changes were spectral diffusion of the peak position within ~3 nm of the equilibrium 682-nm peak, which was explained by energetic disorder of the pigment site energies [29]. However, a rather small percentage of complexes (<5%) were shown to switch reversibly to states characterised by an emission maximum between ~690 nm and ~750 nm appearing in addition to the energetically stable 682-nm band. The switches to these near-infrared states were found to be rather insensitive to the local environment of the complexes and to involve, on average, no evident intensity change — also when employing conditions mimicking qE [45]. Emission at even longer wavelengths – peaking between approximately 760 nm and 795 nm – was occasionally observed [45]. These far-red states were characterised by broad, single bands and weak emission, and were shown to occur more frequently under conditions that mimicked qE [45]. In this work, the two types of red emission states will be referred to as "moderately red" and "far-red" states.

Based on the above-mentioned SM findings, it was suggested that the moderately red states of LHCII trimers are not involved with the mechanism(s) underlying qE. Similar conclusions were drawn from low-temperature *in vitro* bulk studies on LHCII aggregates and purified liposome-embedded trimers, based on the significantly longer fluorescence lifetimes of F700 compared to that of F680 [25,26,55]. Despite these observations, the states associated with F700 have frequently been considered to act as the major energy traps of qE [14,16,19–22], or were suggested to be an intermediate in the quenching process [56] or in the locus of the main qE site [27].

The main purpose of the current study is to look into these discrepant views from an SM perspective: the possible involvement of the low-energy emission states with thermal energy dissipation is examined by investigating the SM fluorescence intensity dynamics of these states for

single, isolated LHCII complexes exposed to different environmental conditions. Considering that the time spent in red states comprises a relatively small fraction, the data sets used in this study were significantly larger than in previous SM studies [29,31,45] in order to decrease statistical uncertainties. The findings indicate that the moderately red states are visited more frequently when the complexes are exposed to qE-related conditions and that most emission appears around 700 nm, but is unrelated to energy dissipation.

2. Materials and methods

2.1. Sample preparation

Isolation and preparation of the samples were the same as reported in a previous study [45]. In short, Vio-enriched LHCII trimers were isolated by iso-electric focusing from PS II particles obtained from dark-adapted spinach leaves [57], while Zea-enriched trimers were obtained from thylakoids pre-treated with 40 mM ascorbate at pH 5.5 [57]. The two samples contained ~0.4–0.7 Vio and ~0.6 Zea per monomer, respectively (see Table 1). The light-harvesting environment was mimicked by solubilising the complexes in 20 mM Hepes at pH 8.0, which also contained 0.03% (w/v) β-dodecyl-maltoside (β-DM) and 1 mM $MgCl_2$. In all experiments, complexes were first allowed to attach to the substrate within this buffer solution, after which the sample cell was flushed with the experimental solution. The experimental (flushing) solution was the same as the light-harvesting solution, except for two variables: a pH of either 8 or 5.5 was used and a detergent concentration of either 0.03% (w/v) or considerably lower. Sodium citrate (15 mM) was added to the flushing solution when using a pH of 5.5, and a detergent-free flushing solution was used to expose complexes to a low detergent concentration. Immobilisation of the complexes prior to flushing with the experimental solution prevented protein aggregation. Standard microscope slides were coated with poly-L-lysine (Sigma) to facilitate surface immobilisation. The flushing buffer contained no detectable traces of oxygen, which was brought about by thorough gassing of N_2 and using a glucose oxidase catalase scavenging system (200 µg/mL glucose oxidase, 7.5 mg/mL glucose, and 35 µg/mL catalase). All measurements were performed at 5 °C in a hermetically sealed cell.

2.2. Single-molecule spectroscopy

The same experimental setup was used as before [45]. Briefly, the excitation source was a 633-nm continuous-wave He–Ne laser (JDS Uniphase). Complexes were excited individually in the centre of a near-diffraction-limited, near-circularly polarised focal volume with a peak intensity of ~250 W/cm². Fluorescence spectra were acquired by dispersing the photons onto a liquid-nitrogen cooled CCD camera (Princeton Instruments, Roper Scientific, Spec10: 100BR). This constituted the only detection channel for most experiments. A second detection channel was employed simultaneously for one set of measurements,

using a 50/50 beamsplitter to direct half the light onto an avalanche photodiode (SPCM-AQR-16, Perkin-Elmer Optoelectronics) for acquiring wavelength-integrated fluorescence counts.

2.3. Data analysis

Fluorescence counts were collected continuously for 60 s and integrated into consecutive time bins of 10 ms and 1 s for intensity and spectral acquisition, respectively, unless specified differently. Data screening was performed as described in [42]. A good data batch was defined as one showing limited irreversible spectral blueing, and for which the complexes in the light-harvesting mimicking environment showed relatively long survival times and relatively stable emission intensities (see [29]). A number of 500–1000 complexes were generally contained in each data set, where typically 5–7 data sets were used for LH- and qE-mimicking conditions and typically 2–3 data sets when one environmental parameter was changed. Error bars reflect standard deviations as the result of differences between data sets, unless where specified otherwise. Single-band spectra were fitted with a skewed Gaussian function [58], while simultaneously fitting the vibrational band with a normal Gaussian. Double-band spectra were fitted using a double skewed Gaussian function in addition to a normal Gaussian fit of the vibrational band. Fitting of the double-band spectra was facilitated by constraining the skewness and full width at half maximum of the blue bands to match those of single-band spectra within the same spectral sequence. Fitting algorithms were based on the Levenberg–Marquardt algorithm in a least-mean-squares optimisation. All calculations were implemented in MATLAB (The MathWorks).

The amount or strength of fluorescence quenching was defined in the conventional way: $k_d = I_U / I_Q - 1$, where I_U and I_Q refer to the fluorescence intensity of a large ensemble of complexes in the unquenched and quenched environments, respectively. This parameter relates to the actual extent of fluorescence quenching $\%Q = 1 - I_Q / I_U$ through $k_d = \%Q / (1 - \%Q)$. Here, the conditions under which light harvesting was mimicked were considered to be the unquenched environment, while qE-related environmental changes represented quenched environments.

3. Results

In this work we examined the properties of the low-energy states of LHCII trimers exposed to different environmental conditions. We were mostly interested in the effects incurred by conditions that are generally associated with qE *in vivo*. To accomplish this, an environment that ensures effective harvesting of light *in vivo* was first mimicked by using Vio-enriched complexes at pH 8.0 and a concentration of 0.03% β-DM. Two qE-related conditions were then investigated, namely an acidic environment (pH 5.5) and a low detergent concentration. In addition, Zea-enriched complexes were used when considering both qE-related conditions simultaneously, thus mimicking the qE state in a SM environment. This will be referred to as the SM qE state. The effect of violaxanthin de-epoxidation, though, was not examined explicitly,

Table 1
Pigment composition of isolated LHCII after sucrose gradient ultracentrifugation.

LHCII	Neo	Vio	Ant	Lut	Zea	DEP	Chl a/b
Vio-enriched	27.0 ± 2.1 (1.09 ± 0.05)	10.3–18.0 ± 1.3 (0.40–0.70 ± 0.05)	0.0	55.0 ± 1.6 (2.2 ± 0.1)	0.0	0.0	1.3 ± 0.1
Zea-enriched	27.0 ± 1.2 (1.09 ± 0.05)	2.0 ± 0.2 (0.08 ± 0.01)	2.0 ± 0.2 (0.08 ± 0.01)	54.0 ± 2.2 (2.1 ± 0.1)	15.0 ± 2.1 (0.6 ± 0.1)	84.0	1.3 ± 0.1

Complexes isolated from photosystem-II-enriched particles [57] obtained from the thylakoids of dark-adapted plants (Vio-enriched) and by prior de-epoxidation of the thylakoids at pH 5.5 in the presence of 40 mM ascorbate (Zea-enriched). Neo, Vio, Ant, Lut, Zea, DEP, and Chl a/b: neoxanthin, violaxanthin, antheraxanthin, lutein, zeaxanthin, de-epoxidation state and chlorophyll a/b ratio. Xanthophyll contents denote means and are expressed as a % of total xanthophyll ± S.E. from four replicates; DEP is (Zea + 0.5 Ant) / (Vio + Zea + Ant) (in %). Data in parentheses are the calculated xanthophyll contents per monomer of protein (molar ratio), assuming that one monomer has 14 Chls and a Chl/xanthophyll ratio of 3.5.
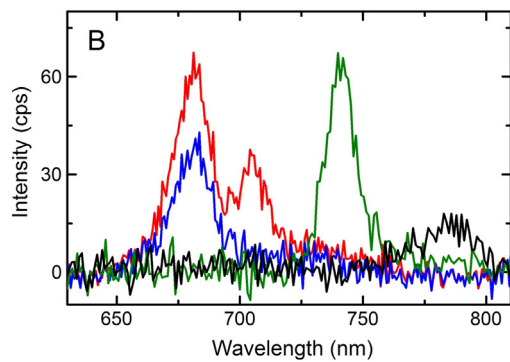
Fig. 1. Four types of SM fluorescence spectra observed from LHCII trimers near room temperature. Intensities denote fluorescence counts per second upon 250 W/cm^2 excitation at 633 nm, without employing normalisation. An integration time of 5 s was used for each spectrum. Spectra in blue and red are from the same complex.

because previous SM studies have shown a small or negligible effect of de-epoxidation [45,46], which was attributed to the detachment of these xanthophylls in a highly diluted environment.

Fig. 1 displays four types of quasi-stable emission spectra of LHCII trimers that have been identified in previous SM studies [29,45]. The most common emission resembles that of the ensemble F680 emission, *i.e.*, peaking at around 682 nm (*blue*). It is important to note that spectra that are blue-shifted by more than ~5 nm originate from denatured or degraded complexes [29] and are not considered here. The states characterised by significantly red-shifted emission were visited reversibly. Of these, the double-band states (*red*) are most prevalent and showed no environmental sensitivity in an earlier study [45], while the occurrence of emission around 780 nm (far-red, *black*) was found to be strongly affected by environmental conditions [45]. The most infrequently occurring red-shifted states are characterised by single-band spectra with emission below 760 nm (*green*) and with properties that resemble those of the red bands of double-band spectra, *i.e.*, narrower and more intense than the far-red spectra. This spectral type will therefore be considered together with the red parts of the double-band spectra.

3.1. Fraction of red emitting complexes

Fig. 2 shows that, on average, the utilised qE-related conditions caused a larger number of complexes to switch into red emission states. The same excitation intensity was used in all experiments, indicating that the observed trend was induced by environmental changes. The effect was particularly large for the far-red states, with as many as 20% of the complexes from a particular sample batch found to exhibit far-red emission within the experimental time in the SM qE environment (though the average value suggests such high values to be rather exceptional). The considerable variation in this number between different data sets is reflected by the sizable error bars and points to the large sensitivity of the far-red states to their local microenvironment. Since these percentages strongly depend on the experimental time frame (a longer time of irradiation increases the probability for a complex to access a low-energy state), a more realistic comparison can be made by considering the relative time spent in a red emission state (Fig. 2, *magenta circles*). This property displayed a similar trend: as more qE-related conditions were added, the average dwell time in low-energy states increased. Comparing the fraction of complexes with the fraction of time in low-energy states it can be deduced that far-red states were on average visited for shorter times than moderately red states, denoting a larger dynamicity of the protein conformations connected to the former.

3.2. Intensity and energy distributions of red states

In order to determine the possible connection between red emission and energy dissipation, we first examined how the average intensity of the different emission bands was affected by the experimental environment. This is shown in Fig. 3A for conditions mimicking the light-harvesting (LH) and qE environments. We distinguished between six types of emission: single-band spectra of complexes exhibiting only emission at around 682 nm (ss), four emission types of complexes exhibiting double-band spectra within the experimental time, and far-red emission. Spectral sequences containing double-band spectra were divided between spectra before and/or after a red state was visited – *i.e.*, single-band spectra peaking at around 682 nm (ds) – and double-band spectra (dd). The blue and red bands of a double-band spectrum

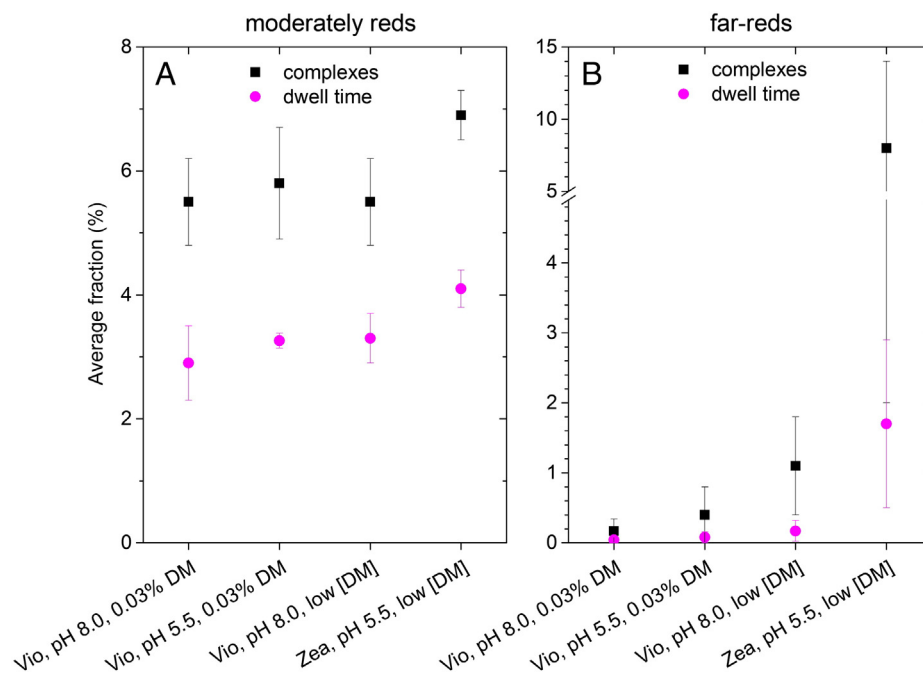**Fig. 2.** Fraction of low-energy states of LHCII trimers in different environments. Percentage of complexes found to exhibit these states (black squares), and fraction of experimental time (magenta circles) in double-band states (A) and single-band, far-red states (B). The discrepancy with the percentages reported in earlier studies [29,45] is due to statistical variations between different sample batches. See text for details.
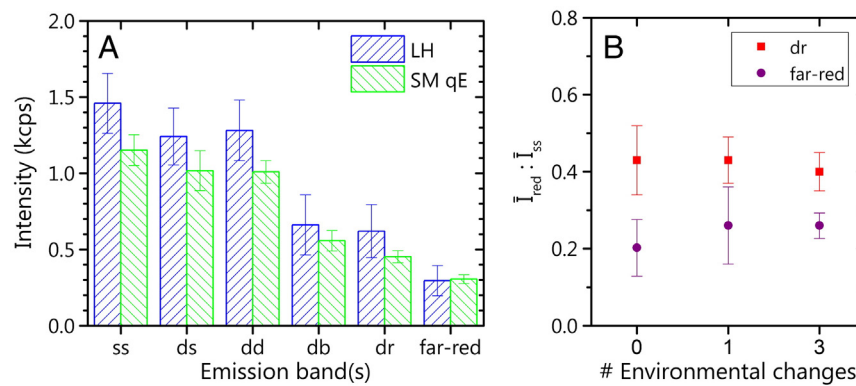
Fig. 3. (A) Average intensity of different types of emission bands for LHCII trimers in LH (blue) and SM qE (green) environments. (B) Intensity ratio between red emission bands (dr and far-red) and single-band spectral sequences (ss). The number of environmental changes is with respect to the LH environment. See text for details.

are denoted by db and dr, respectively, and their intensities were calculated from skewed Gaussian fits (see the Materials and methods section).

In both environments, complexes exhibiting only single-band (~682 nm) emission within the experimental time frame were on average ~15% more fluorescent than those exhibiting also double-band spectra (i.e., ss compared to ds and dd). This suggests that the latter complexes were in a slightly quenched conformation during the time and before a low-energy state was assumed. Note, however, that the switch into a double-band state was accompanied by a negligible intensity change (ds vs. dd), as reported before [45]. Moreover, the comparable intensities of the two bands of double-band states (db vs. dr) indicate that the two associated emission sites were equally populated.

Considering the environmental dependence of the emission, all bands became on average weaker when the LH environment was replaced with a SM qE environment, except the far-red band. Of most interest here was the ratio between the average intensities of the red bands and F680 bands (i.e., $\bar{I}_{dr}$:$\bar{I}_{ss}$ and $\bar{I}_{far-red}$:$\bar{I}_{ss}$) in the different experimental environments, because these intensity ratios are another important factor in determining the relative contribution of red emission in ensemble spectra (the first factor being the relative time spent in red states). In addition, the intensity ratios may also provide information about a possible relationship between the quenching mechanisms underlying the different types of emission. Fig. 3B shows that as more qE-related conditions were added, both $\bar{I}_{dr}$:$\bar{I}_{ss}$ and $\bar{I}_{far-red}$:$\bar{I}_{ss}$ remained constant within the experimental error, while a small increasing trend could also describe the behaviour of the latter. This can be explained by the moderately red emission states being weaker energy traps than the far-red states and qE-associated dissipative F680 states. In other words, the trapping efficiency of the qE-related dissipative states is virtually independent of the sites responsible for F680 and moderately red emission, which is probably the result of many excitonic states being delocalised across a large part of the trimer during energy equilibration [59]. Furthermore, the far-red states, being energy dissipative, would compete with the qE-associated energy traps.

The red emission states were investigated in more detail by resolving their associated peak wavelengths and examining environmentally induced spectral changes. Due to the relatively small changes that are at play, the properties are shown only for the LH and full SM qE environments. Fig. 4 displays the peak wavelength distribution of all the resolved low-energy bands and their corresponding intensity. Evidently, upon replacing the environment, the abundance of far-red states increased considerably. The intensity and energy of the moderately red states occurring in dr-spectra varied across a large scale, and occurrences of emission were found peaking up to ~770 nm, which is further into the infrared than the red-most emission observed in previous studies [29,45]. Two other observations are of interest: (i) by far the most emission occurred at 700 ± 10 nm; and (ii) in the SM qE environment,

the average intensity seems to decrease with λ_m. Both effects are explored in Fig. 5 in more detail.

Fig. 5A confirms that for dr-spectra the majority of low-energy bands peaked at around 700 nm. The distribution around 700 nm became somewhat narrower in the SM qE environment, thus contributing to more pronounced emission at 700 nm. Fig. 5B indicates some specific trends in the average intensity as function of the peak emission: first increasing and then decreasing at longer wavelengths. This behaviour is particularly clear for the SM qE environment, reaching a maximum intensity for an emission peak of ~710 nm. Assuming a distinct emission site for F680 and the red emission, the maximum intensities of the red states per emission site are comparable to or, in the case of the LH environment, even exceeding that of F680. Notably, for the SM qE environment, the intensity of emission beyond ~720 nm showed a larger environmental sensitivity than emission at shorter wavelengths, suggesting the presence of two distinct processes contributing to the moderately red emission.

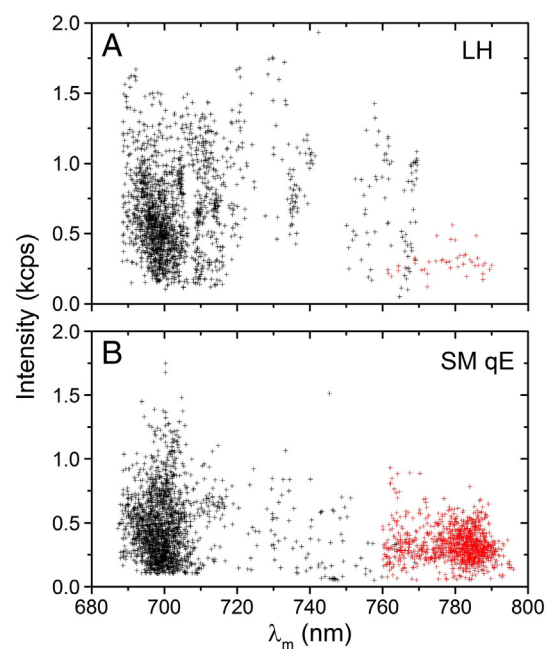**Fig. 4.** Fluorescence peak wavelength (λ_m) and corresponding intensities of red bands for LHCII trimers in environments mimicking the light-harvesting state (A) and qE conditions (B). Black dots refer to the red bands of double-band spectra (dr), and red dots to far-red spectra. Note that the intensity of the black dots is on average only half the total emission of the double bands (dd).
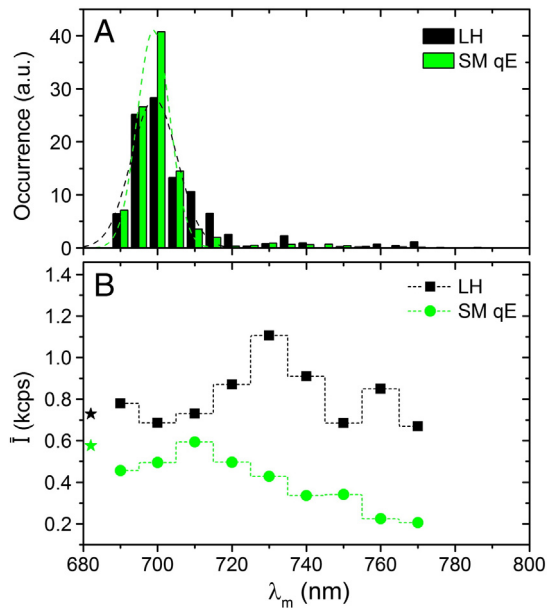
Fig. 5. (A) Peak wavelength distribution of moderately red spectra originating from LHCII trimers exposed to the LH (black) and SM qE (green) conditions. Bins of 5 nm were used and distributions were normalised to the same number of events. Dashed curves denote Gaussian fits of data in the region 700 ± 15 nm. Peak position of both fits was at 699 nm, while full width at half maximum was 14 nm and 10 nm for LH and SM qE conditions, respectively. (B) Average intensity as function of the peak wavelength (λ_m) of moderately red spectra for LH (black) and SM qE (green) conditions. Bins of 10 nm were used. Stars denote half the emission intensity of the F680 state.

3.3. Red emission vs. fluorescence blinking

Fig. 6 provides more information on the relationship between the red emission and fluorescence blinking. Blinking was observed for all types of moderately red states, a representative behaviour of which is shown in Fig. 6A. The intensity fluctuations generally corresponded to

negligible shifts in the emission peak position within the experimental error (Fig. 6B), pointing to distinct processes underlying the intensity and energy switches. Fig. 6C indicates that the average dwell time in quenched states (τ_Q) exhibited the same environmental dependence for the average F680 and average moderately red emission. Taking into account that F700 was the dominant red emission state (Figs. 4 and 5A), it can be deduced from Fig. 3B that the environmentally induced change in the intrinsic brightness was, on average, the same for both F680 and F700 emission states. Hence, blinking affected the emission properties of these two states to a similar degree. However, for moderately red states τ_Q showed a strong wavelength dependence (Fig. 6D), suggesting some involvement of the longer-wavelength states with the mechanism underlying blinking.

3.4. Average SM fluorescence spectra

Fig. 7 shows that the average dwell time in moderately red states exhibited a linear relationship with the extent of environmentally induced quenching. Considering that values of k_d as large as 10 to 20 are often found in literature for in vitro ensemble experiments, the amount of quenching exhibited in the SM qE environment is a large underestimation and very likely also the dwell time in red states. Since the intensity ratio between F680 and F700 was essentially independent of the environment in this study (Figs. 3 and 6C), it is reasonable to extrapolate the linear trend to larger values of k_d. According to this prediction, complexes would spend on average between ~30% and ~60% of their time in double-band states for k_d varying between 10 and 20, so that the contribution of red emission would be between ca. 15% and 30% of the total emission.

Averaging over all the SM spectra in the LH and SM qE environments, the respective ensemble spectra are displayed in Fig. 8A, together with the spectra that we predict on the basis of our analysis for significantly larger values of k_d. The contribution of red emission becomes particularly prominent for larger k_d values. The ensemble average of all experimental red spectra is shown in Fig. 8B for three
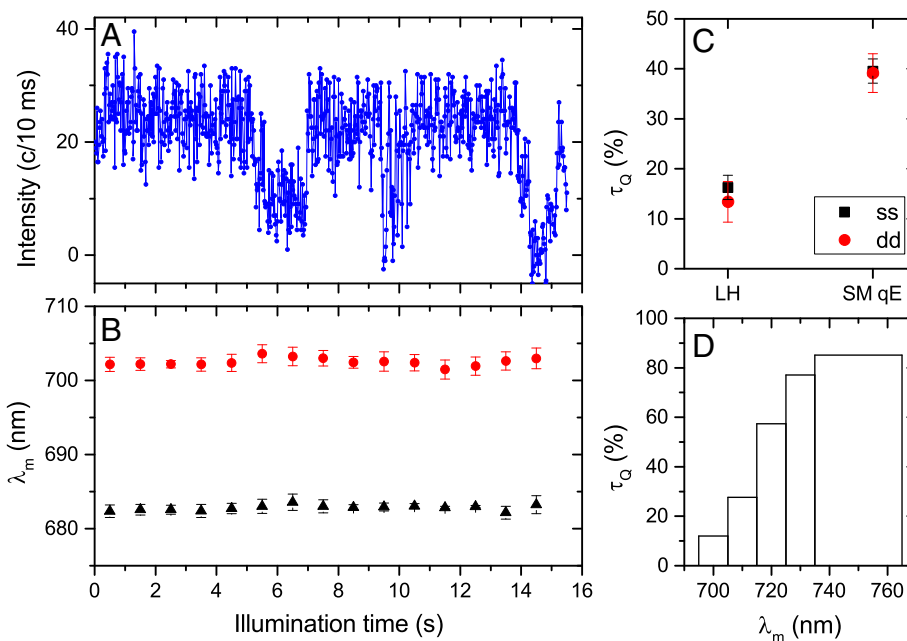
Fig. 6. (A) Example of intensity fluctuations from an LHCII trimer exhibiting a double-band spectrum. Single-step fluctuations between the highest and lowest intensity levels between 9 and 10 s reflect a single quantum unit. (B) Corresponding peak positions of F680 and F700 emission bands for 1 s bins, indicating fitting uncertainties as standard deviations. (C) Dwell time in quenched states for single-band (black) and moderately red emission states (red). Quenched were defined as states corresponding to an intensity of at most 50% of the level of the fully emitting states. (D) Dwell time in quenched states of different spectral states, represented here by their emission peak (λ_m). LHCII trimers were in an LH environment. Bin sizes are reflected by bar widths.

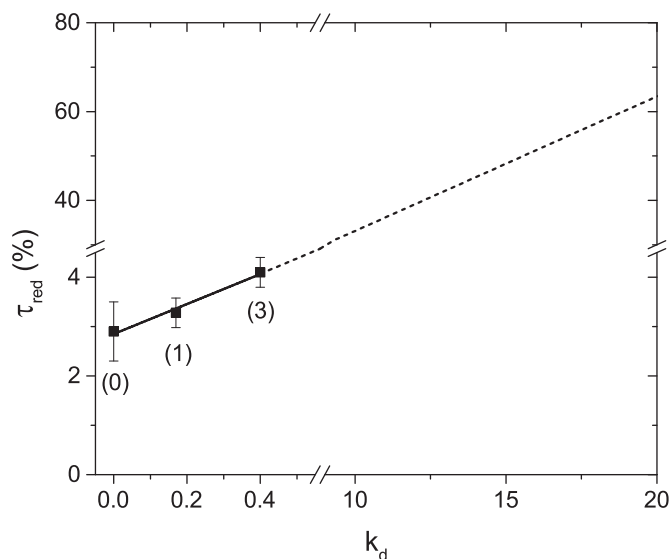**Fig. 7.** Average dwell time in moderately red-shifted states (τ_{red}) as function of the amount of quenching (k_d) induced by different environments. Numbers in parentheses denote number of environmental conditions changed with respect to the LH environment. The linear fit was extrapolated to large k_d values. Here, $k_d = I_U / I_Q - 1$, where I_U and I_Q refer to the ensemble intensity of complexes in the unquenched and quenched environments, respectively.

environmental conditions. In agreement with Fig. 5A, the predominant emission peaked around 700 nm and became more pronounced when the complexes were exposed to a larger number of qE-related conditions. A long red tail extends between ~720 nm and up to 800 nm, including the contribution of the large number of weakly emitting, far-red states.

4. Discussion

4.1. Contribution of red emission states to energy dissipation

The equilibrium shifts to moderately red and far-red states in qE-related environments indicate that when LHCII complexes were exposed to these conditions, their protein energy landscapes allowed the red states to be accessed with a higher probability. However, this

does not necessarily imply that the red states are directly related to the mechanism(s) underlying qE. The results rather suggest that most of the moderately red states are decoupled from thermal energy dissipative states. The relationship between all the types of red states and non-radiative energy dissipation will be discussed here.

First, the observation that all far-red states are weakly emitting indicates that these states decay mostly non-radiatively, thereby quenching a significant fraction of the excitation energy. In addition, qE-related conditions substantially increased the probability of accessing these states, which suggests that the associated energy dissipation pathways may be important avenues to quench excess excitation energy under qE conditions.

Second, the moderately red states showed on average only a weak relationship with energy dissipation. In particular, the largest fraction of states corresponded to emission at 700 ± 10 nm (*i.e.*, F700) and had the same average intensity as the main F680 band, independent of the utilised environments. However, moderately red emission beyond ~720 nm got quenched under SM qE conditions, suggesting a stronger involvement of these states in thermal energy dissipation than the F700 states. Furthermore, the increasing dwell time in moderately red states upon introducing qE-related conditions was significantly smaller than the decrease in the average fluorescence intensity, the latter of which is determined primarily by a shift of the intensity distribution towards quenched states. This suggests that the mechanism underlying fluorescence quenching has a significantly stronger environmental sensitivity than that underlying the appearance of F700 emission.

Several observations point to a disconnection between F700 emission and fluorescence blinking: (i) blinking of red states without accompanying spectral changes (Fig. 6A, B); (ii) the smaller environmentally induced shift into red states than into quenched states (Fig. 2A); (iii) the environmental insensitivity of the intensity ratio of F680 and red states (Fig. 3B), involving both the intrinsic brightness and the average time spent in quenched states (Fig. 6C); and (iv) the disjunction between the switches into moderately red states and quenched states (see, *e.g.*, the comparable intensities of ds and dd in Fig. 3A).

4.2. Relating the red states to those from previous bulk studies

In order to determine the physiological relevance of our findings, the observed properties of LHCII trimers in the utilised SM environments are considered in the context of previous ensemble studies of LHCII. In particular, the average behaviour of thousands of individually measured
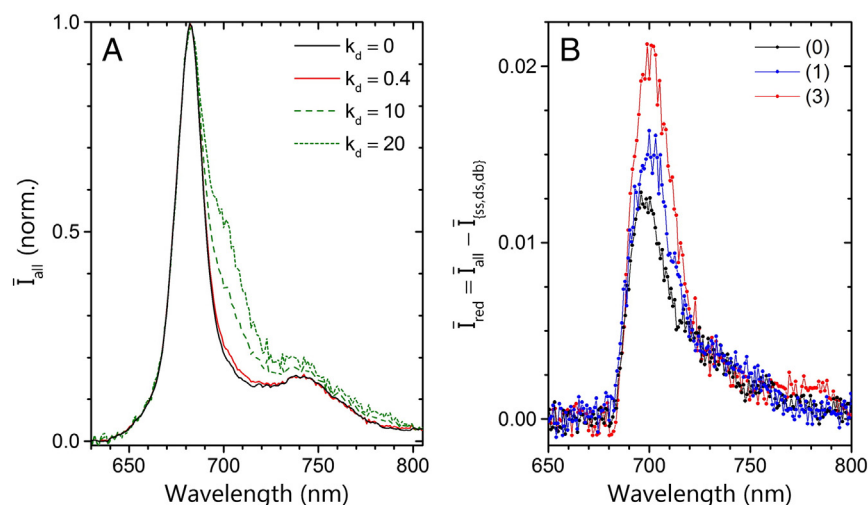
Fig. 8. (A) Time- and population averaged ensemble spectrum of SM spectra acquired under LH conditions ($k_d = 0$) and SM qE conditions ($k_d = 0.4$), as well as predicted spectra for higher k_d values. Spectra are normalised to F680 peak. (B) Time- and population averaged spectrum of all low-energy bands of individually measured LHCII trimers in three different environments. Spectra denote differences between full ensemble (all) and all F680 emission ({ss, ds, db}). Intensities are relative to those in (A). The legend denotes the number of environmental parameters that were changed with respect to the LH environment (black), where (1) refers to a change in pH or detergent (blue), and (3) to a change in pH, detergent, and de-epoxidation state (red).

complexes is compared with the spectroscopic responses of LHCII as revealed by previous *in vitro* and *in vivo* studies.

It should first be noted that the utilised experimental conditions mimicked the physiological environment to a reasonable extent. Under conditions mimicking the *in vivo* light-harvesting state of LHCII trimers, the fluorescence intensity of the unquenched state corresponds remarkably well to the predicted value [29], the ensemble-averaged room-temperature fluorescence spectrum perfectly matches the steady-state ensemble spectrum [29], and the fluorescence lifetime of single, surface-bound LHCII trimers is identical to that of freely diffusing, solubilised trimers in ensemble experiments (J.M. Gruber, personal communication), all of which point to a weak influence of surface binding or other SM-specific parameters. Similarly, the cumulative effect of low detergent, low pH and increased de-epoxidation mimicked qE conditions *in vivo*. Although *in vivo* a pH gradient is present over the membrane, several early studies on the mechanism of qE have clearly demonstrated that by lowering the pH in the incubation medium it is possible to obtain qE quenching (see, *e.g.*, [60,61]). It was found that the same process could be induced in isolated LHCII complexes and is controlled by the xanthophyll cycle [8]. Furthermore, considerable fluorescence quenching was observed from LHCII trimers in a gel matrix with a low detergent content, an arrangement in which neighbouring trimers were well-separated [23,24]. In the latter study the quenched state was related to qE, based on the finding that the accompanying spectroscopic changes corresponded well to those found in chloroplasts and leaves after qE induction. In a low detergent environment, the proteins will likely be slightly compressed due to their hydrophobic surfaces being repelled by water molecules. For LHCII trimers it was demonstrated that even slight compression induces significant thermal energy dissipation [62].

Three groups of low-energy states, each of which is characterised by a different environmental response, are separated in this study, *viz.*, moderately red states peaking near 700 nm, moderately red states peaking beyond ~710 nm, and far-red states (peaking beyond ~760 nm). For all three types of red states, emission states with similar properties were also observed in previous *in vitro* ensemble studies, which strongly suggests that the observed spectral dynamics are not SM-specific phenomena (*i.e.*, induced solely by the SM environment) but are very likely the same changes that occur during qE.

4.2.1. 690–710 nm emission

Although the moderately red states covered a broad energy range, with associated peaks between ~690 nm and up to ~770 nm, the average spectrum consisted of a single, broad band with a maximum at ~700 nm. Taking into account that the latter band was enhanced in a qE-mimicking environment, it may seem reasonable to associate it with the F700 emission band characteristic of aggregated LHCII at 77 K [15–18,26]. Such an association, however, should take into account the temperature dependence of the red emission from aggregates as well as the spectroscopic signature of non-interacting (*i.e.*, well-separated) trimers. First, 700 nm is the characteristic peak position of LHCII aggregates at 77 K, but the peak shifts to beyond 705 nm above 180 K [15,17]. Second, no red emission has as yet been reported for isolated trimers from wild-type plants studied at room temperature using an ensemble approach.

These two considerations can be explained by the above-mentioned aggregates having extensive energy transfer and totally equilibrated pigment pools at higher temperatures [17]. Therefore, at some temperature, the distribution of emitting states in the aggregates will be at a lower energy than the distribution of low-energy states in LHCII trimers. In contrast, LHCII trimers were observed in the same study to exhibit red emission with a peak position that remained essentially constant in the temperature range between 4 K and 180 K [17]. The red emission was too weak to be observed at higher temperatures. The stable fluorescence peak position rules out the possibility of aggregate formation to explain the trimers' low-energy emission. This is confirmed by a more recent

study, where it was shown that controlled quenching of LHCII trimers incorporated into a gel matrix, an arrangement that prevented aggregation, gave rise to weak emission near 700 nm at 77 K [23]. It is therefore very likely that LHCII trimers exhibit a 700-nm emission band also at room temperature, but with intensity too weak to be resolved by the utilised ensemble approaches. This wavelength corresponds perfectly with the dominant 700-nm red emission in the present study (which was conducted near room temperature), and its tiny contribution to the ensemble spectrum can be explained feasibly by the small fraction of time spent in low-energy states (see Fig. 2). This confirms that the qE-related F700 bulk emission is associated with an intrinsic state of a single trimeric complex and not the result of inter-trimer interactions [23]. The formation of protein aggregates will consequently stabilise this pre-existing state by increasing the average dwell time which a complex spends in a red state, a concept that is in line with a widely accepted model of protein functionality [63].

The different components into which the F700 band of LHCII aggregates has been deconvoluted in bulk *in vitro* studies – at least five components [17,26] – can be explained by different realisations of large static disorder of mixed exciton–CT states. Indeed, due to the strong coupling between such mixed states and protein vibrational states (*i.e.*, phonons), their energetic disorder is largely determined by conformational disorder of the highly charged local protein environment. In addition, due to the charged character of CT states, the red states are expected to have a considerably higher tendency to fluctuate energetically than pure excitonic states. The latter property has been illustrated by SM experimental and modelling studies [29,31], site-directed mutagenesis [64], and theoretical studies [65,66].

4.2.2. 710–760 nm emission

A number of room-temperature ensemble studies indicated the presence of emission states with lower energy than the prominent F700 state. For example, time-resolved fluorescence studies of wild-type and mutant *Arabidopsis* leaves after NPQ induction revealed additional emission bands with peak wavelengths extending up to 740 nm, giving rise to an ensemble spectrum with a broad tail between 710 nm and 760 nm [14,20]. In addition, using a homebuilt multiwavelength fluorometer to spectrally resolve the NPQ induction kinetics of *Arabidopsis* leaves, a 720-nm emission band was resolved at room temperature [67]. It was suggested that these bands are the hypsochromically shifted F700 low-temperature band of aggregates [14,67], although it can be inferred from an early temperature-dependence study on LHCII aggregates that above 180 K the peak of the low-energy band does not extend far beyond ~710 nm [17]. A more reasonable interpretation is based on a steady-state study on spinach and *Arabidopsis* leaves [13], where it was shown that ~740-nm emission does not reflect a new, physical state but result from reabsorption of scattered fluorescence, which causes a strong enhancement of the vibronic band in the 710–760 nm window. However, a clear emission band near 740 nm was observed from the poikilohydric lichens *Parmelia* and *Physciella*, assigned to PS II, and shown to be weak for samples in the hydrated state but considerably enhanced in the desiccated state [68–70]. Although no direct connection between the desiccation-related signals and the plant NPQ-related signals has as yet been found, it is likely that 720–740 nm emission states are similarly intrinsic to plant PS II at physiological temperatures, although with a low probability of access. Indeed, a recent 77 K Stark fluorescence spectroscopy study on LHCII aggregates has provided evidence for the presence of two distinct low-energy qE-related states, with associated emission bands peaking at 696 nm and 713–715 nm, respectively [27]. The latter finding supports the observation in the present study that ~700-nm emission states showed a different response to qE-related environmental conditions than states with longer wavelengths. In the Stark fluorescence study, the 696-nm band was found to be accompanied by small contributions peaking at 714 nm and 755 nm, thereby clearly confirming the presence of distinct emission states beyond 710 nm [27].

We propose that a significant fraction of the emission beyond 710 nm observed in the above-mentioned ensemble studies originates from the same site within LHCII as the red states between 710 nm and 760 nm of the present study. The energy of the associated exciton–CT hybrid state is expected to vary significantly due to conformationally induced disorder, giving rise to quasi-stable sub-populations under certain environmental conditions. In particular, under light-harvesting conditions these states have a very small probability to be accessed, but small protein structural distortions due to desiccation, mutation, aggregation, or the onset of qE may enhance some of the sub-populations. This would, for example, explain the varying amplitudes of the extensively red-shifted room-temperature decay-associated spectra of aggregated LHCII trimers isolated from *Arabidopsis* mutants with different Vio and Zea contents [14].

4.2.3. >760 nm emission

In a former SM study [45] it was proposed that the far-red emission might be related to the above-mentioned 713–715 nm Stark fluorescence band. However, the current study suggests that this Stark band is rather related to the 710–760 nm spectra, while the far-red emission denotes a distinct spectral state with different associated energy dissipation properties. This idea is supported by a very recent line-narrowing study at 8 K, where it was found that far-red emission states with very similar spectral properties occur in the PS II core complexes of plants (spinach) and cyanobacteria (*Thermosynechococcus vulcanus*) [71]. The peaks of the far-red states were resolved to be between 770 nm and 790 nm, the emission was weak, and the spectra were extensively broadened. This finding provides strong support for the idea that the far-red emission from LHCII trimers observed in SM studies is not related to artefacts. We propose that the ~780-nm state is intrinsic to all PS II pigment–protein complexes.

4.3. Likely sites of the red emission

It was shown above that the F700 emission states show no relationship with fluorescence blinking. A complete disconnection of the underlying processes most readily occurs when they originate from different sites in the complex and by means of different molecular mechanisms. Former SM experimental and computational studies provided different lines of evidence to relate the primary mechanisms underlying qE and fluorescence blinking for isolated LHCII trimers, where it was assumed that the major component of qE occurs in these complexes [45–48]. In this work we similarly adopt the view that qE conditions considerably increase the probability of energy transfer from the terminal emitter Chls to the S_1 state of Lut 1 [36]. We have, furthermore, provided motivations for relating the F700 emission in this study to the characteristic red emission that occurs under qE conditions. It thus follows that the site of the characteristic qE-related F700 emission is not in the locus of Lut 1, in contrast to previous claims based on bulk *in vitro* studies [14,27,67,72]. Comparison with the SM spectral dynamics of Lhca complexes provides strong evidence that most of LHCII's moderately red emission originates from the Lut 2 domain: the characteristic emission of Lhca complexes strongly resembles LHCII's moderately red states in various respects, exhibiting a double-band spectrum, with the redder peak occurring typically between ~690 nm and ~730 nm and which can diffuse energetically and be switched off reversibly [31]. There is substantial evidence that the red emission originates from a mixed exciton–CT state of the Chl dimer 603–609 in the Lut 2 site [32,33,73,74]. Considering the spectral similarity and the strong structural and compositional homology between LHCII and the Lhca complexes, it is very likely that most of the F700 emission of LHCII (peaking between ~690 and ~710 nm) originates from the Chl dimer $a603–b609$ in the Lut 2 site.

In contrast to the F700 emission states, the states associated with peaks between 710 nm and 760 nm showed some correlation with energy dissipation, in agreement with the above-mentioned Stark fluorescence study where the 713–715 nm band was observed to be weaker than the 696 nm band and thus more strongly connected to energy dissipation [27]. We therefore propose that the 710–760 nm emission is related to fluorescence blinking and thus to the primary mechanism of qE, which we assume to be located in the Lut 1 site. The similarity between the spectral shapes of all moderately red spectra suggests a similar origin, *i.e.*, a mixed exciton–CT state formed among two or more Chls. In the Lut 1 site this would involve the strongly coupled Chl $a610–a611–a612$ cluster.

The environmentally induced shifts to far-red states and blinking-related quenched states were qualitatively similar, strongly suggesting some relationship between the underlying processes. However, the intensity of the far-red states showed a different response to environmental changes than the F680 emission intensity, indicating different underlying energy-dissipation mechanisms. Since fluorescence blinking is accompanied by minor or no spectral shifts, only relatively small conformational changes are likely involved with this phenomenon [45]. This agrees with the observation from several bulk *in vitro* studies that access to the qE state involves only subtle conformational changes [24,75,76]. We therefore propose that the relationship between far-red emission and fluorescence quenching points to their underlying mechanisms operating in the same locus, both involving Lut 1. More specifically, if the S_1 state of Lut 1 forms a CT state and mixes with one or more of the lowest Chl exciton states, significantly red-shifted spectra will be observed. Access to such a mixed state will particularly be promoted when the Lut S_1 state couples more strongly to the Q_y state of one or more of its neighbouring Chls. Such coupling was found to be strongly correlated with the extent of qE [34,77]. In addition, the non-radiative character of the Lut S_1 state is expected to reduce the emission when this state forms an exciton–CT hybrid state with Chl. This would explain the comparatively small intensity of the far-red states compared to that of moderately red states, considering the latter to originate from exciton–CT hybrid states among Chls. Furthermore, for two molecules with disparate transition energies the low-energy states are expected to have a larger CT component, resulting in an exciton–CT state with a lower energy. Involvement of a CT state would also explain the strong environmental sensitivity of the far-red states, which was found to vary significantly between different experiments using the same batch of sample.

4.4. Support from literature for decoupling the moderately red states and quenched states

Disentangling the site of the dominant low-energy emission states (F700) from the site of the primary energy dissipative states is not only supported by this study but also can explain a number of findings from previous *in vitro* bulk studies.

(i) In a very recent steady-state fluorescence study, a particular point mutation of the LHCII protein (replacing glutamate 94 with glycine) resulted in the complex's quenched state having no associated red-shifted emission under qE-related conditions [78]. Although the quenching capability was somewhat reduced by the mutation, the results demonstrate that considerable energy dissipation can occur in LHCII without any characteristic low-energy emission. (ii) High levels of quenching were induced for LHCII trimers immobilised in a solid-state gel, though the extents of the accompanying red shifts were rather small, leading to ensemble peak positions between 680 and 690 nm [23]. This finding is in contrast to the characteristic strong emission band at 700 nm observed from aggregates and suggests a rather weak correlation between energy dissipation and low-energy states. (iii) Related to the previous finding are the observations from several studies that the major LHCII and minor antenna complexes exhibited different relationships between the extent of quenching and the extent of the accompanying red shift [55,79–82]. (iv) Based on early time-resolved studies of LHCII aggregates at 80 K it was proposed that none of the resolved red-shifted states is directly involved in the quenching mechanism [25,26]. The decay-associated spectra resolved in the latter studies indicated
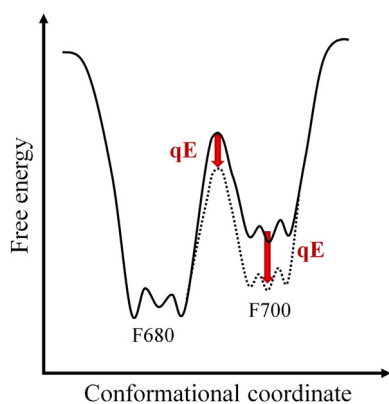
Fig. 9. Scheme of simplified protein energy landscape, illustrating how qE conditions may change the landscape to increase both the rate of accessing an F700 state and the average dwell time in such a state. Dashed curves denote part of landscape after qE induction. The two large local minima correspond to the conformation related to ~680-nm and ~700-nm emission, respectively.

that the different transient species decayed into one another, where consecutive components had an increasingly longer wavelength and a corresponding increasingly longer lifetime. A similar behaviour was found for LHCII trimers incorporated into liposomes [55].

Disconnecting the sites responsible for low-energy emission and non-radiative energy dissipation does not oppose the bulk *in vitro* observations that upon quenching, some red emission does generally occur. This can be explained by considering the conformational change that accompanies the switch into a quenched state to not be localised in the Lut 1 locus but to affect the conformational landscape in the Lut 2 domain such that a red emission state can be accessed with a higher probability. This is illustrated conceptually in Fig. 9, showing that the qE-related conformational change lowers the free-energy barrier between the conformational substates associated with F680 and F700 emission. The reduced free energy of the F700 conformation reflects stabilisation of this state under qE conditions. It is of note that the high packing density of the LHCII protein [11] would not likely allow

conformational changes to be localised but instead to affect a significant part of the protein structure. This would explain the configurational twist of Neo in LHCII under qE conditions, indicative of a protein conformational change, though the molecular change itself is likely not part of the qE mechanism [24,36]. It was demonstrated for a structurally homologous protein (Lhca4 in PS I) that a small structural change as the result of a point mutation has a very large effect on the spectroscopic properties of its pigments, in particular when a mixed exciton–CT state is involved [64].

4.5. The role of environmentally controlled conformational disorder

The disconnected intensity and energy fluctuations signify that several processes can act at the same time at different sites upon a single LHCII complex. Our findings indicate that the F700 state and quenched F680 state correspond to distinct conformations and that qE conditions shift the population equilibrium into both states simultaneously, as illustrated in Fig. 10. As indicated, the F680 state preceding a moderately red state is slightly quenched, and the F700 state also frequently switches into a quenched state. Switching between the four emission states in Fig. 10 points to intrinsic protein conformational disorder, while the population equilibrium, which is controlled by the complex's local environment, determines in which state the complex is on average. As such, conformational disorder is environmentally controlled to regulate the functionality of the complexes, in particular the extent of energy dissipation. This concept affirms the hypothesis for qE proposed more than 20 years ago [83] and refined later [84,85].

The simultaneous population shift to quenched states and the F700 state under qE conditions leads to a quite remarkable conclusion: that qE makes LHCII look spectrally more like Lhca. Indeed, it was proposed that Lhca and Lhcb complexes can be approximated by a single generic protein structure, such that the F680 and F700 states are intrinsic to the disordered energy landscape of this protein [31]. By controlling the disorder of the protein microenvironment in the Lut 2 site, the population distribution between the two states can be controlled, associating Lhca to a stable F700 conformation and Lhcb to a stable F680 conformation.
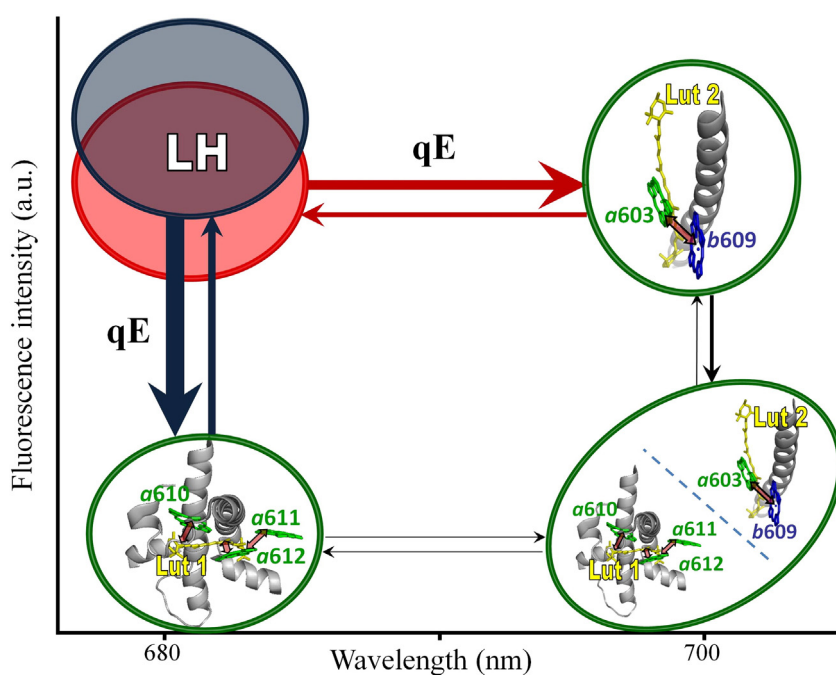

Fig. 10. Model illustrating the two main qE-induced population shifts (two thickest arrows in blue and red) and the likely sites of primary thermal energy dissipation and ~700-nm emission. The monomeric structure and nomenclature of Ref. [37] were used and the qE-mechanism of Ref. [36] is assumed. LH denotes the light-harvesting state, characterised by ~680-nm emission and assumes a different average intensity for the two main switches. The arrow thickness gives a qualitative indication of the frequency of occurrence of a particular conformational change.

5. Summary

We have illustrated the value of using SM approaches to study a complex phenomenon like qE. SM spectroscopy adds considerable dynamical information, elucidating protein dynamics, revealing new emission states, and illustrating the important role of protein conformational disorder.

The different spectral states of LHCII can be categorised into four groups, with peak emission at approximately 680–685 nm, 690–710 nm, 710–760 nm, and >760 nm, respectively, based on their responses to qE-related environmental changes. We propose that each of these spectral groups, with the exception of F700 (*i.e.*, spectra with peaks at 690–710 nm), is closely associated with a distinct qE mechanism, and that environmentally controlled disorder determines the relative contributions of the different emissive states. Within each of the three groups of red-shifted states, the emission wavelength can fluctuate considerably because of ample (though small-scale) conformational disorder of the local protein environments. Energetically invariant blinking (associated with 680–685 nm fluorescence) was shown to contribute to the largest amount of energy dissipation, followed by far-red states (with >760 nm emission maximum) under qE-related conditions, and only weak quenching associated with the 710–760 nm moderately red states.

The results clearly show that F700 is the most abundant moderately red state under the utilised conditions but not involved with energy dissipation, despite the observation that it is accessed more frequently under conditions mimicking qE. Disentangling F700 from the dominant qE state, and thus separating the respective sites of origin, can explain numerous findings from previous *in vitro* bulk studies. The characteristic appearance of a F700 band under quenching conditions in bulk *in vitro* and *in vivo* experiments without the associated states being involved with the dominant qE mechanism was explained by the conformational switch into the energy-dissipating state increasing the probability of conformational switching into a low-energy state. Therefore, changes in the Lut 1 domain – the proposed major site of thermal energy dissipation – are such that quenching may occur *via* a mixture of physical processes dependent perhaps on the very small difference in the perturbation of the Chl and Lut molecules.

Acknowledgments

References

[1] R. Croce, H. van Amerongen, Light-harvesting and structural organization of photosystem II: from individual complexes to thylakoid membrane, J. Photochem. Photobiol. B Biol. 104 (2011) 142–153.

[2] R. van Grondelle, J.P. Dekker, T. Gillbro, V. Sundstrom, Energy-transfer and trapping in photosynthesis, Biochim. Biophys. Acta Bioenerg. 1187 (1994) 1–65.

[3] R. van Grondelle, V.I. Novoderezhkin, Energy transfer in photosynthesis: experimental insights and quantitative models, Phys. Chem. Chem. Phys. 8 (2006) 793–807.

[4] B. Demmig-Adams, W.W. Adams, U. Heber, S. Neimanis, K. Winter, A. Kruger, F.C. Czygan, W. Bilger, O. Bjorkman, Inhibition of zeaxanthin formation and of rapid changes in radiationless energy-dissipation by dithiothreitol in spinach leaves and chloroplasts, Plant Physiol. 92 (1990) 293–301.

[5] X.P. Li, A.M. Gilmore, S. Caffarri, R. Bassi, T. Golan, D. Kramer, K.K. Niyogi, Regulation of photosynthetic light harvesting involves intrathylakoid lumen pH sensing by the PsbS protein, J. Biol. Chem. 279 (2004) 22866–22874.

[6] R.G. Walters, A.V. Ruban, P. Horton, Higher plant light-harvesting complexes LHCIIa and LHCIIc are bound by dicyclohexylcarbodiimide during inhibition of energy dissipation, Eur. J. Biochem. 226 (1994) 1063–1069.

[7] M.P. Johnson, T.K. Goral, C.D.P. Duffy, A.P.R. Brain, C.W. Mullineaux, A.V. Ruban, Photoprotective energy dissipation involves the reorganization of photosystem ii light-harvesting complexes in the grana membranes of spinach chloroplasts, Plant Cell 23 (2011) 1468–1479.

[8] P. Horton, A.V. Ruban, R.G. Walters, Regulation of light harvesting in green plants, Annu. Rev. Plant Physiol. Plant Mol. Biol. 47 (1996) 655–684.

[9] A.V. Ruban, M.P. Johnson, C.D.P. Duffy, The photoprotective molecular switch in the photosystem II antenna, Biochim. Biophys. Acta Bioenerg. 1817 (2012) 167–181.

[10] J. Zaks, K. Amarnath, E.J. Sylak-Glassman, G.R. Fleming, Models and measurements of energy-dependent quenching, Photosynth. Res. 116 (2013) 389–409.

[11] T. Barros, A. Royant, J. Standfuss, A. Dreuw, W. Kuhlbrandt, Crystal structure of plant light-harvesting complex shows the active, energy-transmitting state, EMBO J. 28 (2009) 298–306.

[12] G.S. Beddard, G. Porter, Concentration quenching in chlorophyll, Nature 260 (1976) 366–367.

[13] M.P. Johnson, A.V. Ruban, Photoprotective energy dissipation in higher plants involves alteration of the excited state energy of the emitting chlorophyll(s) in the light harvesting antenna II (LHCII), J. Biol. Chem. 284 (2009) 23592–23601.

[14] Y. Miloslavina, A. Wehner, P.H. Lambrev, E. Wientjes, M. Reus, G. Garab, R. Croce, A.R. Holzwarth, Far-red fluorescence: a direct spectroscopic marker for LHCII oligomer formation in non-photochemical quenching, FEBS Lett. 582 (2008) 3625–3631.

[15] A.V. Ruban, P. Horton, Mechanism of [Delta]pH-dependent dissipation of absorbed excitation energy by photosynthetic membranes. I. Spectroscopic analysis of isolated light-harvesting complexes, Bioenergetics 1102 (1992) 30–38.

[16] A.V. Ruban, D. Rees, G.D. Noctor, A. Young, P. Horton, Long-wavelength chlorophyll species are associated with amplification of high-energy-state excitation quenching in higher-plants, Biochim. Biophys. Acta 1059 (1991) 355–360.

[17] A.V. Ruban, J.P. Dekker, P. Horton, R. Vangrondelle, Temperature-dependence of chlorophyll fluorescence from the light-harvesting complex II of higher-plants, Photochem. Photobiol. 61 (1995) 216–221.

[18] J.E. Mullet, C.J. Arntzen, Simulation of grana stacking in a model membrane system — mediation by a purified light-harvesting pigment–protein complex from chloroplasts, Biochim. Biophys. Acta 589 (1980) 100–117.

[19] W.I. Gruszecki, E. Janik, R. Luchowski, P. Kernen, W. Grudzinski, I. Gryczynski, Z. Gryczynski, Supramolecular organization of the main photosynthetic antenna complex LHCII: a monomolecular layer study, Langmuir 25 (2009) 9384–9391.

[20] A.R. Holzwarth, Y. Miloslavina, M. Nilkens, P. Jahns, Identification of two quenching sites active in the regulation of photosynthetic light-harvesting studied by time-resolved fluorescence, Chem. Phys. Lett. 483 (2009) 262–267.

[21] M. Zubik, R. Luchowski, W. Grudzinski, M. Gospodarek, I. Gryczynski, Z. Gryczynski, J.W. Dobrucki, W.I. Gruszecki, Light-induced isomerization of the LHCII-bound xanthophyll neoxanthin: possible implications for photoprotection in plants, Biochim. Biophys. Acta Bioenerg. 1807 (2011) 1237–1243.

[22] M. Zubik, R. Luchowski, M. Puzio, E. Janik, J. Bednarska, W. Grudzinski, W.I. Gruszecki, The negative feedback molecular mechanism which regulates excitation level in the plant photosynthetic complex LHCII: towards identification of the energy dissipative state, Biochim. Biophys. Acta Bioenerg. 1827 (2013) 355–364.

[23] C. Ilioaia, M.P. Johnson, P. Horton, A.V. Ruban, Induction of efficient energy dissipation in the isolated light-harvesting complex of photosystem II in the absence of protein aggregation, J. Biol. Chem. 283 (2008) 29505–29512.

[24] A.A. Pascal, Z.F. Liu, K. Broess, B. van Oort, H. van Amerongen, C. Wang, P. Horton, B. Robert, W.R. Chang, A. Ruban, Molecular basis of photoprotection and control of photosynthetic light-harvesting, Nature 436 (2005) 134–137.

[25] C.W. Mullineaux, A.A. Pascal, P. Horton, A.R. Holzwarth, Excitation-energy quenching in aggregates of the LHC-II chlorophyll–protein complex — a time-resolved fluorescence study, Biochim. Biophys. Acta 1141 (1993) 23–28.

[26] S. Vasilev, K.D. Irrgang, T. Schrotter, A. Bergmann, H.J. Eichler, G. Renger, Quenching of chlorophyll alpha fluorescence in the aggregates of LHCII: steady state fluorescence and picosecond relaxation kinetics, Biochemistry 36 (1997) 7503–7512.

[27] M. Wahadoszamen, R. Berera, A.M. Ara, E. Romero, R. van Grondelle, Identification of two emitting sites in the dissipative state of the major light harvesting antenna, Phys. Chem. Chem. Phys. 14 (2012) 759–766.

[28] J. Pieper, J. Voigt, G. Renger, G.J. Small, Analysis of phonon structure in line-narrowed optical spectra, Chem. Phys. Lett. 310 (1999) 296–302.

[29] T.P.J. Krüger, V.I. Novoderezhkin, C. Ilioaia, R. van Grondelle, Fluorescence spectral dynamics of single LHCII trimers, Biophys. J. 98 (2010) 3093–3101.

[30] V.I. Novoderezhkin, J.P. Dekker, R. Van Grondelle, Mixing of exciton and charge-transfer states in photosystem II reaction centers: modeling of Stark spectra with modified Redfield theory, Biophys. J. 93 (2007) 1293–1311.

[31] T.P.J. Krüger, E. Wientjes, R. Croce, R. van Grondelle, Conformational switching explains the intrinsic multifunctionality of plant light-harvesting complexes, Proc. Natl. Acad. Sci. U. S. A. 108 (2011) 13516–13521.

[32] R. Croce, A. Chojnicka, T. Morosinotto, J.A. Ihalainen, F. van Mourik, J.P. Dekker, R. Bassi, R. van Grondelle, The low-energy forms of photosystem I light-harvesting complexes: spectroscopic properties and pigment–pigment interaction characteristics, Biophys. J. 93 (2007) 2418–2428.

[33] E. Romero, M. Mozzo, I.H.M. van Stokkum, J.P. Dekker, R. van Grondelle, R. Croce, The origin of the low-energy form of photosystem I light-harvesting complex Lhca4: mixing of the lowest exciton with a charge-transfer state, Biophys. J. 96 (2009) L35–L37.

[34] S. Bode, C.C. Quentmeier, P.N. Liao, N. Hafi, T. Barros, L. Wilk, F. Bittner, P.J. Walla, On the regulation of photosynthesis by excitonic interactions between carotenoids and chlorophylls, Proc. Natl. Acad. Sci. U. S. A. 106 (2009) 12311–12316.

[35] P.N. Liao, C.P. Holleboom, L. Wilk, W. Kuhlbrandt, P.J. Walla, Correlation of Car S-1 → Chl with Chl → Car S-1 energy transfer supports the excitonic model in quenched light harvesting complex II, J. Phys. Chem. B 114 (2010) 15650–15655.

[36] A.V. Ruban, R. Berera, C. Ilioaia, I.H.M. van Stokkum, J.T.M. Kennis, A.A. Pascal, H. van Amerongen, B. Robert, P. Horton, R. van Grondelle, Identification of a mechanism of photoprotective energy dissipation in higher plants, Nature 450 (2007) 575–578.

[37] Z. Liu, H. Yan, K. Wang, T. Kuang, J. Zhang, L. Gui, X. An, W. Chang, Crystal structure of spinach major light-harvesting complex at 2.72 A resolution, Nature 428 (2004) 287–292.

[38] T.K. Ahn, T.J. Avenson, M. Ballottari, Y.C. Cheng, K.K. Niyogi, R. Bassi, G.R. Fleming, Architecture of a charge-transfer state regulating light harvesting in a plant antenna protein, Science 320 (2008) 794–797.

[39] T.J. Avenson, T.K. Ahn, D. Zigmantas, K.K. Niyogi, Z. Li, M. Ballottari, R. Bassi, G.R. Fleming, Zeaxanthin radical cation formation in minor light-harvesting complexes of higher plant antenna, J. Biol. Chem. 283 (2008) 3550–3558.

[40] N.E. Holt, D. Zigmantas, L. Valkunas, X.P. Li, K.K. Niyogi, G.R. Fleming, Carotenoid cation formation and the regulation of photosynthetic light harvesting, Science 307 (2005) 433–436.

[41] U. Gerken, H. Wolf-Klein, C. Huschenbett, B. Gotze, S. Schuler, F. Jelezko, C. Tietz, J. Wrachtrup, H. Paulsen, Single molecule spectroscopy of oriented recombinant trimeric light harvesting complexes of higher plants, Single Mol. 3 (2002) 183–188.

[42] T.P.J. Krüger, C. Ilioaia, R. Van Grondelle, Fluorescence intermittency from the main plant light-harvesting complex: resolving shifts between intensity levels, J. Phys. Chem. B 115 (2011).

[43] C. Tietz, F. Jelezko, U. Gerken, S. Schuler, A. Schubert, H. Rogl, J. Wrachtrup, Single molecule spectroscopy on the light-harvesting complex II of higher plants, Biophys. J. 81 (2001) 556–562.

[44] T.P.J. Krüger, C. Ilioaia, L. Valkunas, R. Van Grondelle, Fluorescence intermittency from the main plant light-harvesting complex: sensitivity to the local environment, J. Phys. Chem. B 115 (2011).

[45] T.P.J. Krüger, C. Ilioaia, M.P. Johnson, A.V. Ruban, E. Papagiannakis, P. Horton, R. van Grondelle, Controlled disorder in plant light-harvesting complex II explains its photoprotective role, Biophys. J. 102 (2012) 2669–2676.

[46] T.P.J. Krüger, C. Ilioaia, M.P. Johnson, E. Belgio, P. Horton, A.V. Ruban, R. Van Grondelle, The specificity of controlled protein disorder in the photoprotection of plants, Biophys. J. 105 (2013) 1018–1026.

[47] J. Chmeliov, L. Valkunas, T.P.J. Krueger, C. Ilioaia, R. van Grondelle, Fluorescence blinking of single major light-harvesting complexes, New J. Phys. 15 (2013).

[48] L. Valkunas, J. Chmeliov, T.P.J. Krüger, C. Ilioaia, R. van Grondelle, How photosynthetic proteins switch, J. Phys. Chem. Lett. 3 (2012) 2779–2784.

[49] M. Brecht, V. Radics, J.B. Nieder, R. Bittl, Protein dynamics-induced variation of excitation energy transfer pathways, Proc. Natl. Acad. Sci. U. S. A. 106 (2009) 11857–11861.

[50] L.-N. Liu, A.T. Elmalk, T.J. Aartsma, J.-C. Thomas, G.E.M. Lamers, B.-C. Zhou, Y.-Z. Zhang, Light-induced energetic decoupling as a mechanism for phycobilisome-related energy dissipation in red algae: a single molecule study, PLoS One 3 (2008).

[51] D. Loos, M. Cotlet, F. De Schryver, S. Habuchi, J. Hofkens, Single-molecule spectroscopy selectively probes donor and acceptor chromophores in the phycobiliprotein allophycocyanin, Biophys. J. 87 (2004) 2598–2608.

[52] J.B. Nieder, M. Brecht, R. Bittl, Dynamic intracomplex heterogeneity of phytochrome, J. Am. Chem. Soc. 131 (2009) 69–71.

[53] D. Rutkauskas, J. Olsen, A. Gall, R.J. Cogdell, C.N. Hunter, R. van Grondelle, Comparative study of spectral flexibilities of bacterial light-harvesting complexes: structural implications, Biophys. J. 90 (2006) 2463–2474.

[54] A.M. van Oijen, M. Ketelaars, J. Kohler, T.J. Aartsma, J. Schmidt, Unraveling the electronic structure of individual photosynthetic pigment–protein complexes, Science (New York, N.Y.) 285 (1999) 400–402.

[55] I. Moya, M. Silvestri, O. Vallon, G. Cinque, R. Bassi, Time-resolved fluorescence analysis of the photosystem II antenna proteins in detergent micelles and liposomes, Biochemistry 40 (2001) 12552–12561.

[56] M.G. Mueller, P. Lambrev, M. Reus, E. Wientjes, R. Croce, A.R. Holzwarth, Singlet energy dissipation in the photosystem ii light-harvesting complex does not involve energy transfer to carotenoids, ChemPhysChem 11 (2010) 1289–1296.

[57] A.V. Ruban, P.J. Lee, M. Wentworth, A.J. Young, P. Horton, Determination of the stoichiometry and strength of binding of xanthophylls to the photosystem II light harvesting complexes, J. Biol. Chem. 274 (1999) 10458–10465.

[58] R.B.D Fraser, E. Suzuki, Resolution of overlapping bands: functions for simulating band shapes, Anal. Chem. 41 (1969) 37–39.

[59] V.I. Novoderezhkin, A. Marin, R. van Grondelle, Intra- and inter-monomeric transfers in the light harvesting LHCII complex: the Redfield–Förster picture, Phys. Chem. Chem. Phys. 13 (2011) 17093–17103.

[60] A. Krieger, I. Moya, E. Weis, Energy-dependent quenching of chlorophyll-a fluorescence — effect of pH on stationary fluorescence and picosecond-relaxation kinetics in thylakoid membranes and photosystem-II preparations, Biochim. Biophys. Acta 1102 (1992) 167–176.

[61] D. Rees, G. Noctor, A.V. Ruban, J. Crofts, A. Young, P. Horton, pH dependent chlorophyll fluorescence quenching in spinach thylakoids from light treated or dark adapted leaves, Photosynth. Res. 31 (1992) 11–19.

[62] B. van Oort, A. van Hoek, A.V. Ruban, H. van Amerongen, Equilibrium between quenched and nonquenched conformations of the major plant light-harvesting complex studied with high-pressure time-resolved fluorescence, J. Phys. Chem. B 111 (2007) 7631–7637.

[63] D.D. Boehr, R. Nussinov, P.E. Wright, The role of dynamic conformational ensembles in biomolecular recognition, Nat. Chem. Biol. 5 (2009) 789–796.

[64] E. Wientjes, G. Roest, R. Croce, From red to blue to far-red in Lhca4: how does the protein modulate the spectral properties of the pigments? Biochim. Biophys. Acta Bioenerg. 1817 (2012) 711–717.

[65] T. Renger, Theory of optical spectra involving charge transfer states: dynamic localization predicts a temperature dependent optical band shift, Phys. Rev. Lett. 93 (2004).

[66] S. Vaitekonis, G. Trinkunas, L. Valkunas, Red chlorophylls in the exciton model of photosystem I, Photosynth. Res. 86 (2005) 185–201.

[67] P.H. Lambrev, M. Nilkens, Y. Miloslavina, P. Jahns, A.R. Holzwarth, Kinetic and spectral resolution of multiple nonphotochemical quenching components in Arabidopsis leaves, Plant Physiol. 152 (2010) 1611–1624.

[68] M. Komura, A. Yamagishi, Y. Shibata, I. Iwasaki, S. Itoh, Mechanism of strong quenching of photosystem II chlorophyll fluorescence under drought stress in a lichen, Physciella melanchla, studied by subpicosecond fluorescence spectroscopy, Biochim. Biophys. Acta Bioenerg. 1797 (2010) 331–338.

[69] C. Slavov, M. Reus, A.R. Holzwarth, Two different mechanisms cooperate in the desiccation-induced excited state quenching in Parmelia lichen, J. Phys. Chem. B 117 (2013) 11326–11336.

[70] J. Veerman, S. Vasil'ev, G.D. Paton, J. Ramanauskas, D. Bruce, Photoprotection in the lichen Parmelia sulcata: the origins of desiccation-induced fluorescence quenching, Plant Physiol. 145 (2007) 997–1005.

[71] J. Morton, J. Hall, P. Smith, A. Fusamichi, K. Faisal, J.R. Shen, E. Krausz, Determination of the PS I content of PS II core preparations using selective emission: a new emission of PS II at 780 nm, Biochim. Biophys. Acta Bioenerg. 1837 (2014) 167–177.

[72] M.G. Muller, P. Lambrev, M. Reus, E. Wientjes, R. Croce, A.R. Holzwarth, Singlet energy dissipation in the photosystem II light-harvesting complex does not involve energy transfer to carotenoids, ChemPhysChem 11 (2010) 1289–1296.

[73] J.A. Ihalainen, M. Ratsep, P.E. Jensen, H.V. Scheller, R. Croce, R. Bassi, J.E.I. Korppi-Tommola, A. Freiberg, Red spectral forms of chlorophylls in green plant PSI — a site-selective and high-pressure spectroscopy study, J. Phys. Chem. B 107 (2003) 9086–9093.

[74] T. Morosinotto, J. Breton, R. Bassi, R. Croce, The nature of a chlorophyll ligand in Lhca proteins determines the far red fluorescence emission typical of photosystem I, J. Biol. Chem. 278 (2003) 49223–49229.

[75] C. Ilioaia, M.P. Johnson, P.-N. Liao, A.A. Pascal, R. van Grondelle, P.J. Walla, A.V. Ruban, B. Robert, Photoprotection in plants involves a change in lutein 1 binding domain in the major light-harvesting complex of photosystem II, J. Biol. Chem. 286 (2011) 27247–27254.

[76] M. Wentworth, A.V. Ruban, P. Horton, Thermodynamic investigation into the mechanism of the chlorophyll fluorescence quenching in isolated photosystem II light-harvesting complexes, J. Biol. Chem. 278 (2003) 21845–21850.

[77] P.-N. Liao, S. Pillai, M. Kloz, D. Gust, A.L. Moore, T.A. Moore, J.T.M. Kennis, R. van Grondelle, P.J. Walla, On the role of excitonic interactions in carotenoid–phthalocyanine dyads and implications for photosynthetic regulation, Photosynth. Res. 111 (2012) 237–243.

[78] E. Belgio, C.D.P. Duffy, A.V. Ruban, Switching light harvesting complex II into photoprotective state involves the lumen-facing apoprotein loop, Phys. Chem. Chem. Phys. 15 (2013) 12253–12261.

[79] A.V. Ruban, A.J. Young, P. Horton, Dynamic properties of the minor chlorophyll a/b binding proteins of photosystem II, an in vitro model for photoprotective energy dissipation in the photosynthetic membrane of green plants, Biochemistry 35 (1996) 674–678.

[80] M. Wentworth, A.V. Ruban, P. Horton, Chlorophyll fluorescence quenching in isolated light harvesting complexes induced by zeaxanthin, FEBS Lett. 471 (2000) 71–74.

[81] M. Wentworth, A.V. Ruban, P. Horton, Kinetic analysis of nonphotochemical quenching of chlorophyll fluorescence. 2. Isolated light-harvesting complexes, Biochemistry 40 (2001) 9902–9908.

[82] A.V. Ruban, P. Pesaresi, U. Wacker, K.D.J. Irrgang, R. Bassi, P. Horton, The relationship between the binding of dicyclohexylcarbodiimide and quenching of chlorophyll fluorescence in the light-harvesting proteins of photosystem II, Biochemistry 37 (1998) 11586–11591.

[83] P. Horton, A.V. Ruban, D. Rees, A.A. Pascal, G. Noctor, A.J. Young, Control of the light-harvesting function of chloroplast membranes by aggregation of the LHCII chlorophyll protein complex, FEBS Lett. 292 (1991) 1–4.

[84] P. Horton, M.P. Johnson, M.L. Perez-Bueno, A.Z. Kiss, A.V. Ruban, Photosynthetic acclimation: does the dynamic structure and macro-organisation of photosystem II in higher plant grana membranes regulate light harvesting states? FEBS J. 275 (2008) 1069–1079.

[85] P. Horton, M. Wentworth, A. Ruban, Control of the light harvesting function of chloroplast membranes: the LHCII-aggregation model for non-photochemical quenching, FEBS Lett. 579 (2005) 4201–4206.